LOW ENERGY PROTON DAMAGE EFFECTS IN SILICON AND GALLIUM ARSENIDE SOLAR CELLS

by D. M. Brown
NASA, Goddard Space Flight Center, Md.

SUMMARY

Silicon N/P cells of various base resistivities and gallium arsenide P/N solar cells were irradiated with nominally 0.6, 1.8 and 4.7 Mev protons. In the first experiment silicon N/P cells of various base resistivities and gallium arsenide cells were irradiated with 4.7 Mev proton, measuring Isc and V open as functions of flux. In the second experiment, the same types of cells were irradiated with 0.6 Mev protons, with I-V curves and spectral responses being measured. In the third experiment, a similar set of cells were irradiated with 1.8 Mev protons, with I-V curve and spectral response being measured.

INTRODUCTION

This paper presents some results of proton irradiations of silicon N/P solar cells of various base resistivities and gallium arsenide P/N solar cells with low energy protons of various energies, to compare the damage effect of the different types of cells. An unusual anealing effect was found to happen for 10 and 38 ohms cm N/P silicon cells that had been irradiated with 0.6 Mev protons.

PROCEDURE

The Naval Research Laboratory 5-Mev Van de Graaff accelerator was used for the source of protons. In this accelerator, the protons travel down a horizontal drift tube which is approximately 25 ft. long and has a 2 inch inner diameter. Four gold foils, 0.1

mil thick for the 4.7 Mev experiment, were placed 15 ft. from the sample chamber. Nickel foil 0.075 mil thick was used in the 1.8 Mev and 0.6 Mev tests. The foil served to reduce the intensity of the beam and make it uniform.

(Insert Figure 1)

Proton flux was measured with a guarded Faraday cup in the position of the specimen holder, before and after irradiations at the three different energies. At this time the ratio of the flux collected by the cup and the insulated drift tube was determined. During each irradiation the flux collected by the insulated drift tube was used as a measure of the flux incident on the specimens. Cells were 1 cm x 1 cm in size, having been cut in half by a diamond saw.

The Xenon Arc intensity was calibrated with a 12 junction thermopyle at the position of the speciment holder before and after each irradiation; the thermopyle was compared to a normal incidence pyrheliometer, before and after the experiment with the Xenon Arc as the source. The standard intensity was 67mw/cm^2, measured at the cell position. A set of (11) Balzer's interference filters were used to give monochromatic light for the spectral response measurements. The spectral intensity was measured with the 12 junction thermopyle before and after each spectral response measurement.

RESULTS

The following table shows the critical flux $\emptyset_c$ of each of the type of cells used, their efficiency under Xenon Arc and sunlight,

and their initial open circuit voltage. (Table 1)

Table 2 is a listing of the particle penetration depths into the solar cells tested.

(Insert Table 2 and 3)

Figure 2 compares the damage effect of 4.7 Mev protons to a short circuit current ratios of Si N/P 1, 10, and 38 ohm cm cells, and GaAs cells. It will be noted that GaAs and the higher resitivity Si cells have a larger critical flux than the 1 ohm-cm cells, but after an integrated flux of 4 to 8 x $10^{12} p^+ cm^{-2}$, they become worse than the 1 ohm-cm cells.

Figure 3 compares the depreciation of the open circuit voltage for the above cells, under 4.7 Mev proton bombardment.

Figure 4 compares the short circuit current depreciation due to 1.8 Mev protons. The radiation damage does not appear as severe as with the 4.7 Mev protons.

Figure 5 compares the open circuit voltage depreciation of Si 1, 10, and 100 ohm-cm cells, and GaAs cells due to the 1.8 Mev proton flux. The Si 10 ohm-cm cells voltage changed the largest amount of all the cells with the 1.8 Mev protons, as was the case for the 4.7 Mev protons.

Though the apparent critical flux for 1.8 Mev protons is 5.6×10^{12} $p^+ cm^{-2}$ for short circuit current for the GaAs cell, some junction damage effect seems to have taken place at fluxes greater than 5×10^{10}.

Figure 6 shows a comparison of maximum power ratios for 1.8 Mev protons damage, for silicon N/P 1, 10 and 100 ohm-cm cells. The

order of critical flux for the maximum power ratios are the same as it is for the short circuit current ratios, considering just the silicon cells. (Viz, the 1 ohm-cm cell depreciates fastest, the 10 ohm-cm cell next, and least, the 100 ohm-cm cell). In making calculations of radiation damage to a solar array aboard a spacecraft in the radiation belts one must consider the depreciation of the maximum power point of the cell, not the short circuit current.

Figure 7 compares the short circuit current ratios of Silicon N/P 1, 10 and 38 ohm-cm cells and GaAs cells, under 0.6 Mev proton bombardment. The order of critical fluxes are the same as under the 4.7 and 1.8 Mev proton bombardment. A pronounced anealing or recovery effect is seen for the silicon cells, for fluxes greater than $5 \times 10^{12} p^+/cm^2$. This is not seen for the GaAs cell. This will be discussed further when the quantum yield curves are considered.

Depreciation of the open circuit voltage 1, 10 and 38 ohm-cm Si N/P cells, and GaAs cells under 0.6 Mev proton bombardment is shown in Figure 8. For fluxes above $10^{12} p^+/cm^2$, 10 ohm-cm cell depreciates less than the other cells.

Figures 9, 10, 11 and 12 compare the short circuit current ratios for the silicon N/P 1, 10 and 38 ohm-cm cells and GaAs cells, for the protons and in this experiment. The data was replotted to show the variations of the short circuit current of each type cell with proton bombardment energy on a single graph.

Figure 13 shows the variation of the quantum yield of a silicon N/P 1 ohm-cm cell under 0.6 Mev proton bombardment . As is expected

the response in the red drops off rapidly. The broad peak of the curve is typical of high efficiency blue shifted cells.

Figure 14 shows the variation of the quantum yield of a silicon N/P 10 ohm-cm cell, under 0.6 Mev proton bombardment. Marked changes to the junction characteristics and skin response are seen for the $10^{13} p^+/cm^2$ curve. (Attributing the blue response essentially to the skin, n. layer.) The appearance of the peaks in the 10^{13} curve for .77μ and 1.0[illegible] μ light is unexplained. The decrease of the diffusion length of the minority carrier in the skin would not account for the increase in the RED response. Also unexplained is the sharp drop in blue response from 10^{12} to 10^{13} p^+/cm^2.

Figure 15 shows the variation in quantum yield of a silicon N/P 38 ohm-cm cell, under 0.6 Mev proton bombardment. Here also, are marked changes seen between the 10^{12} and 10^{13} p^+/cm^2 bombardments. The peak in the 10^{13} p^+/cm^2 curve is at .8 μ, the same apparant place as it is for the unbombarded cell.

Figure 16 shows the variation in quantum yield of a GaAs P/N cell, under 0.6 Mev proton bombardment. No recovery effects were seen in the short circuit current ratios for this type cell; none is seen here in the quantum yield curve.

Table 2 lists the approximate proton penetration depths for the types of cells used in this test.

CONCLUSION

Unusual recovery effects were shown to happen for the silicon

N/P 10 and 38 ohm-cm cells under 0.6 Mev bombardment, for fluxes greater than $5 \times 10^{12} p^+/cm^2$. A flattening out of the damage rate is seen for Si/ohm-cm cells, for .6 Mev fluxes greater than 5×10^{12} p^+/cm^2. An attempt to analize the radiation damage as being purely due to decrease in diffusion length was felt useless for the 1.8 Mev and 0.6 Mev bombardments because of the short penetration depths. (Standard methods e.g. Baicker and Faughnan (1), require that the particle penetrate the cell at least to a couple of diffusion lengths.) That the particle penetrates only, on the average 37 μ, in the case of 1.8 Mev protons in silicon, or 7.4 μ for 0.6 Mev protons in Si, means that the "diffusion length" in the base region of a cell is not a well defined object. Knock-on protons certainly will contribute to radiation damage, as long as their energy is greater than the dislocation energy (98 ev for protons in Si), but their effect is not uniform to a depth several times the bombarding protons penetration depth.

For previous work, the reader is referred to the article by Wysoki (2) and Weller and Statler (3).

Refr. (1) J. A. Baicker and B. W. Faughnan, "Radiation Induced Changes in Silicon Photovoltaic Cells", J. Applied Physics 33 #11, Nov. 1962.

Refr. (2) J. J. Wysoki "Radiation Studies in GaAs and Si Devices", IEEE, Trans. PTGNS Vol NS-10, #5, Nov. 1963.

Refr. (3) J. F. Weller and R. L. Statler, "Low Energy Proton Damage to Solar Cells", ibid (2)

Table 1

	Efficiency, %		V_{open}	ϕ_c, Critical Fluxes, Multiply nos. below by $10^{10} p^+ cm^{-2}$				
	Xenon	Sun	initial	0.6Mev P^+	1.8Mev P^+		4.7Mev P^+	
Si 1 ohm-cm	9.5-10.5	9.5-10.5	56mv	6.2	21	8.4 (P_{max})	6.6	
Si 10 ohm-cm	10-12	10-12	52mv	18.2	56	18 (P_{max})	12.5	
Si 38 ohm-cm	5		46mv	43			34	
Si 100 ohm-cm	5		44mv	25	120	35 (P_{max})		
GaAs	6-7.5		83-92mv	25	560		560	
					(a)	(b)		

Note:

1) The 10 ohm-cm cells were made by Heliotek; all the rest were RCA.
2) All the Silicon solar cells tested were N/P type; the GaAs cells were P/N.
3) Above, under the 1.8Mev heading , are two columns sublabled (a)for critical flux for the short circuit current, (b)for critical flux for max power ratios.
4) The critical fluxes for the 0.6 and the 4.7 Mev protons is for short circuit current ratios.

Table 2

Proton Penetration Depths (in microns)

Mat'l	0.6Mev	1.8Mev	4.7Mev
Silicon	7.4	37.7	180
Gallium Arsenide	3.5	17.7	84.6

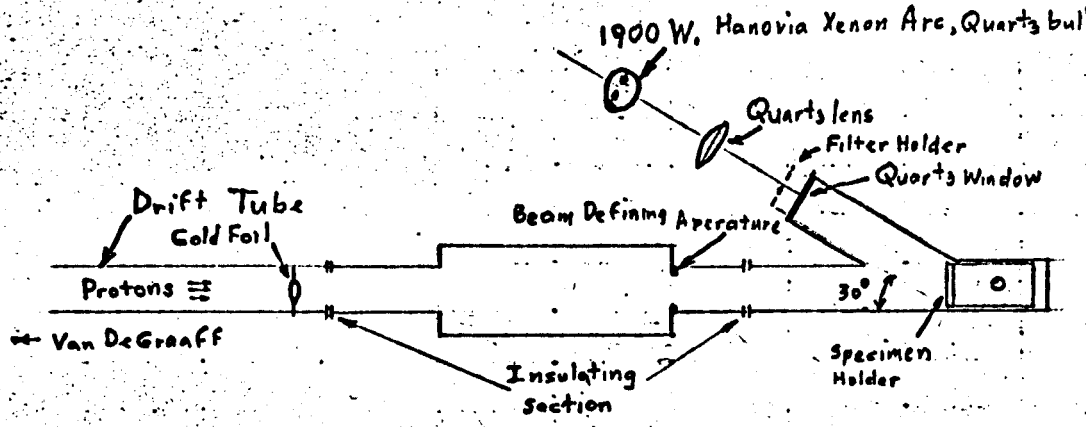

Experimental Arrangement

D.M. Brown
7/12/64

Fig. 1

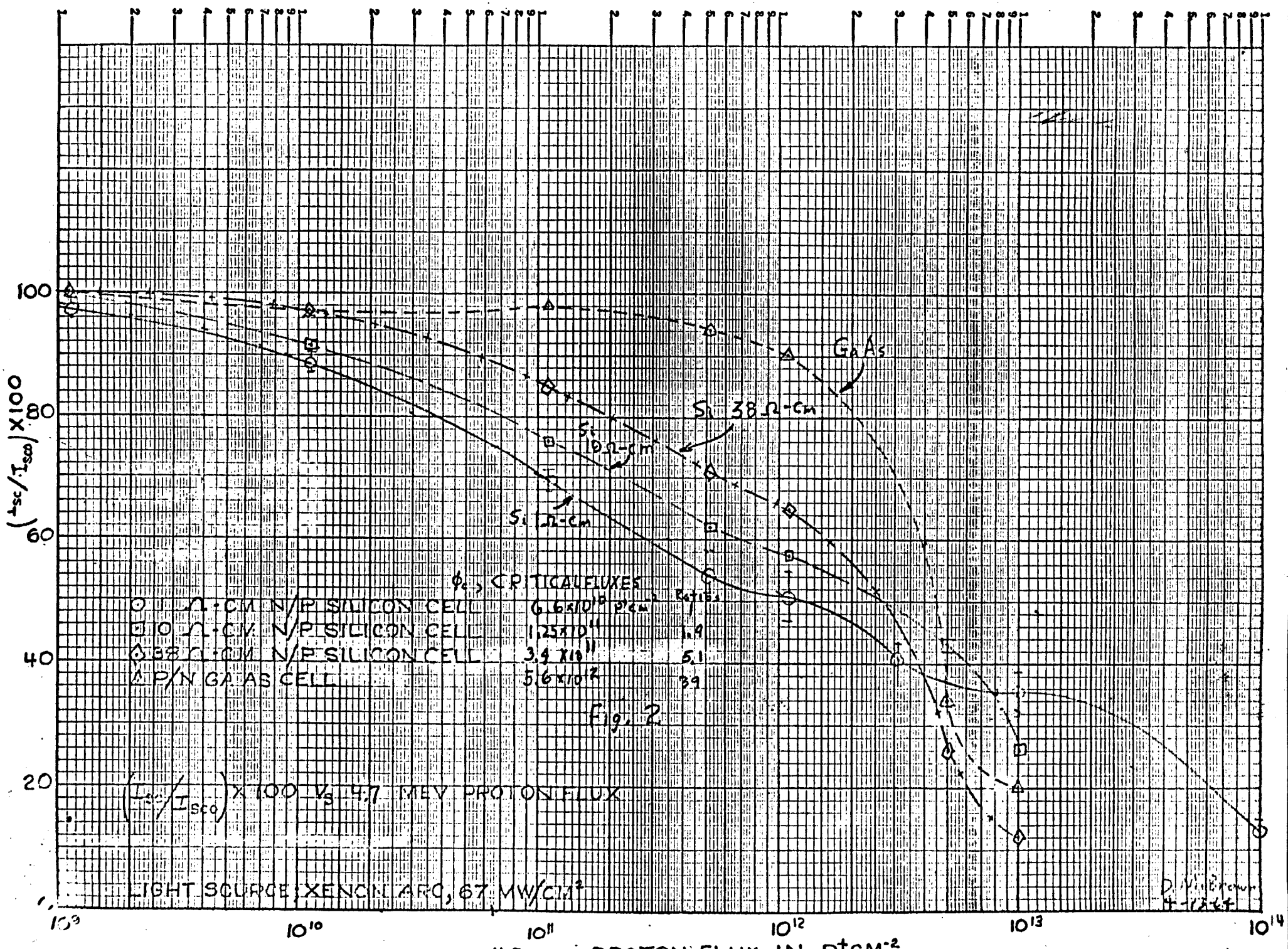

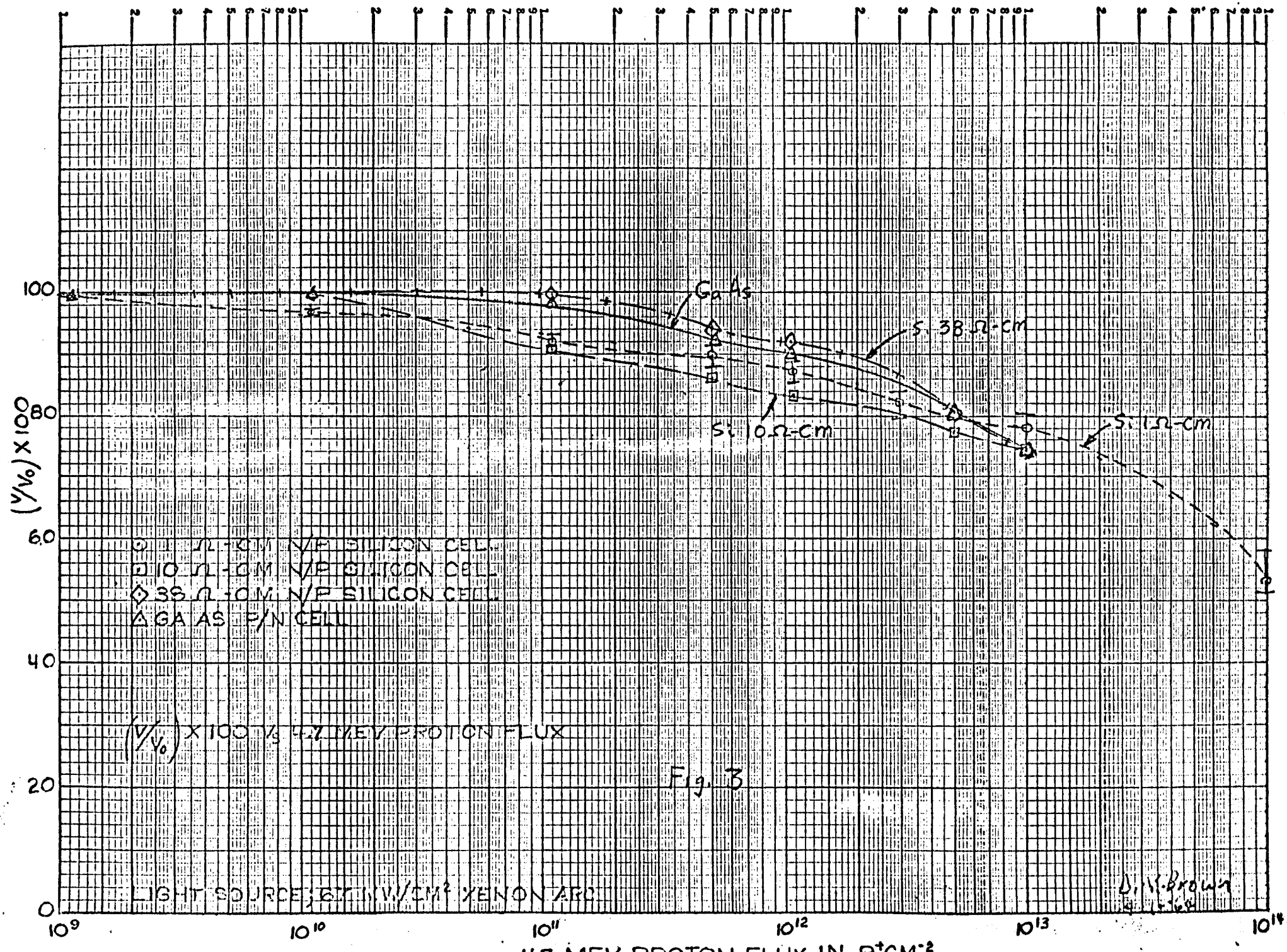

Fig. 3

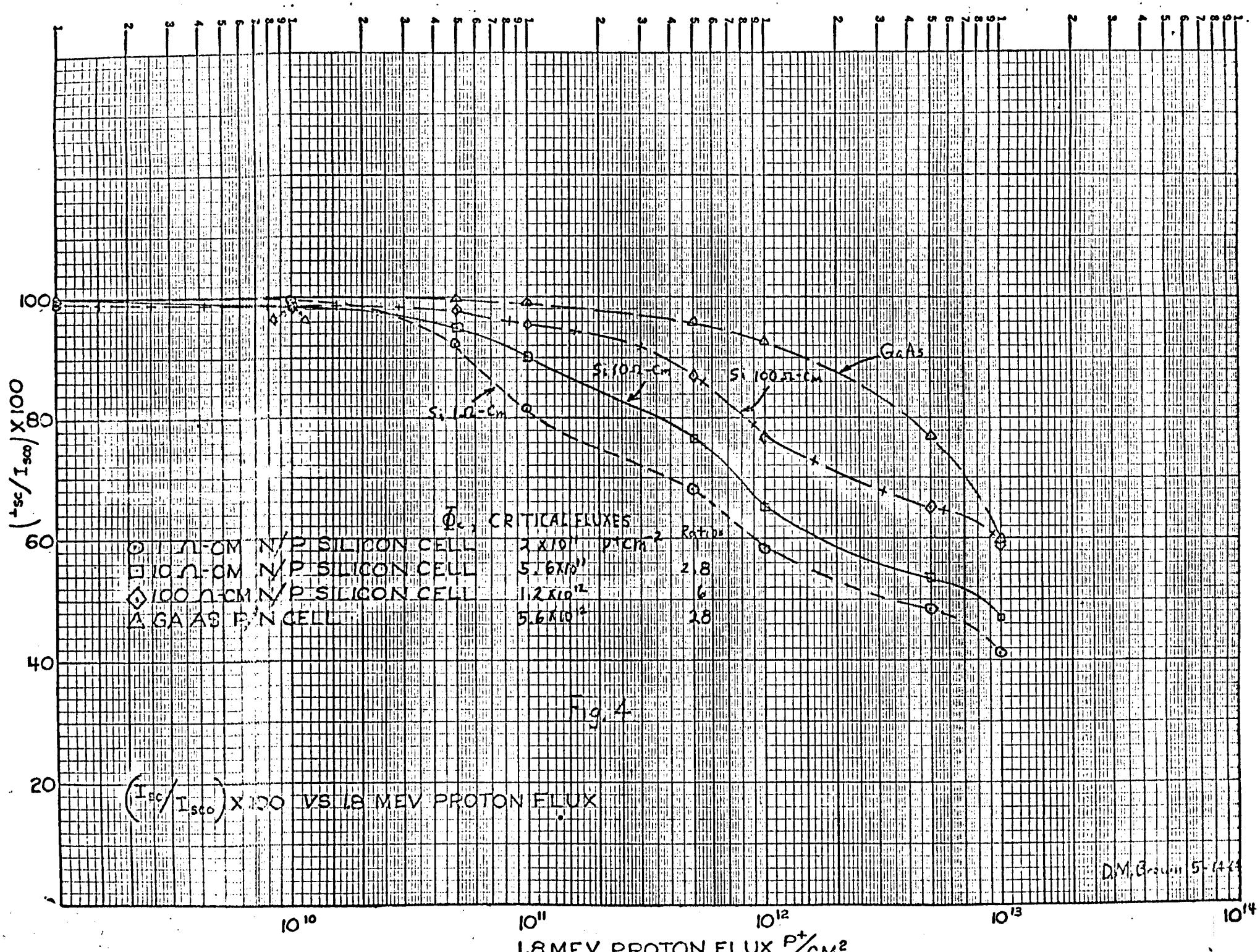

Fig. 4

(I_{sc}/I_{sco}) X 100 VS 1.8 MEV PROTON FLUX

D.M. Brown 5-17-63

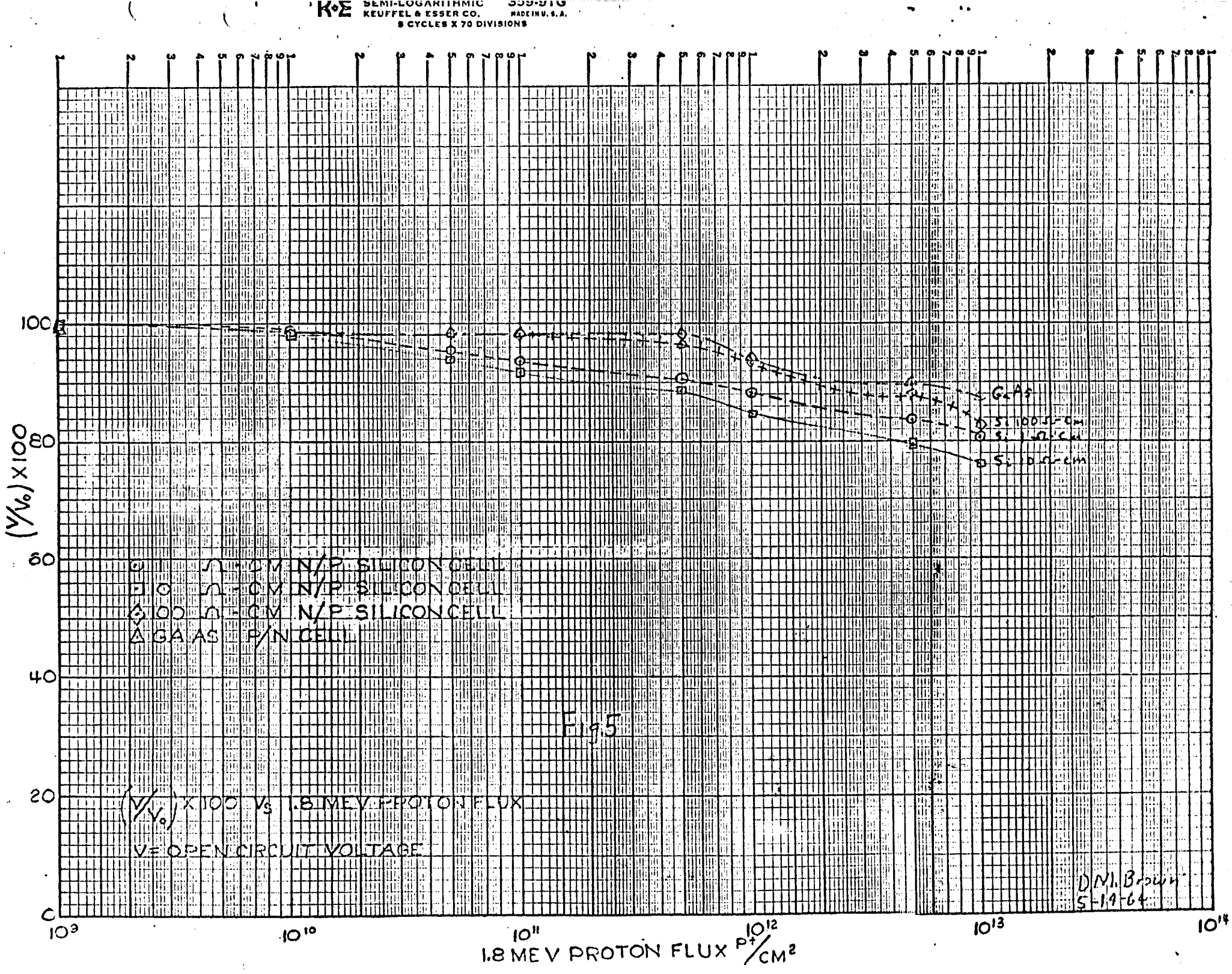
K&E SEMI-LOGARITHMIC 359-91G
KEUFFEL & ESSER CO. MADE IN U.S.A.
3 CYCLES X 70 DIVISIONS
100
80
60
40
20
0
(V/Vo) X 100
10 Ω-CM N/P SILICON CELL
2 Ω-CM N/P SILICON CELL
100 Ω-CM N/P SILICON CELL
GA AS P/N CELL
(V/Vo) X 100 Vs 1.8 MEV PROTON FLUX
V = OPEN CIRCUIT VOLTAGE
GaAs
Si 100 Ω-cm
Si 1 Ω-cm
Si 10 Ω-cm
10^9
10^10
10^11
10^12
10^13
10^14
1.8 MEV PROTON FLUX P+/CM²
D.N. Brown
5-19-64

Fig 5

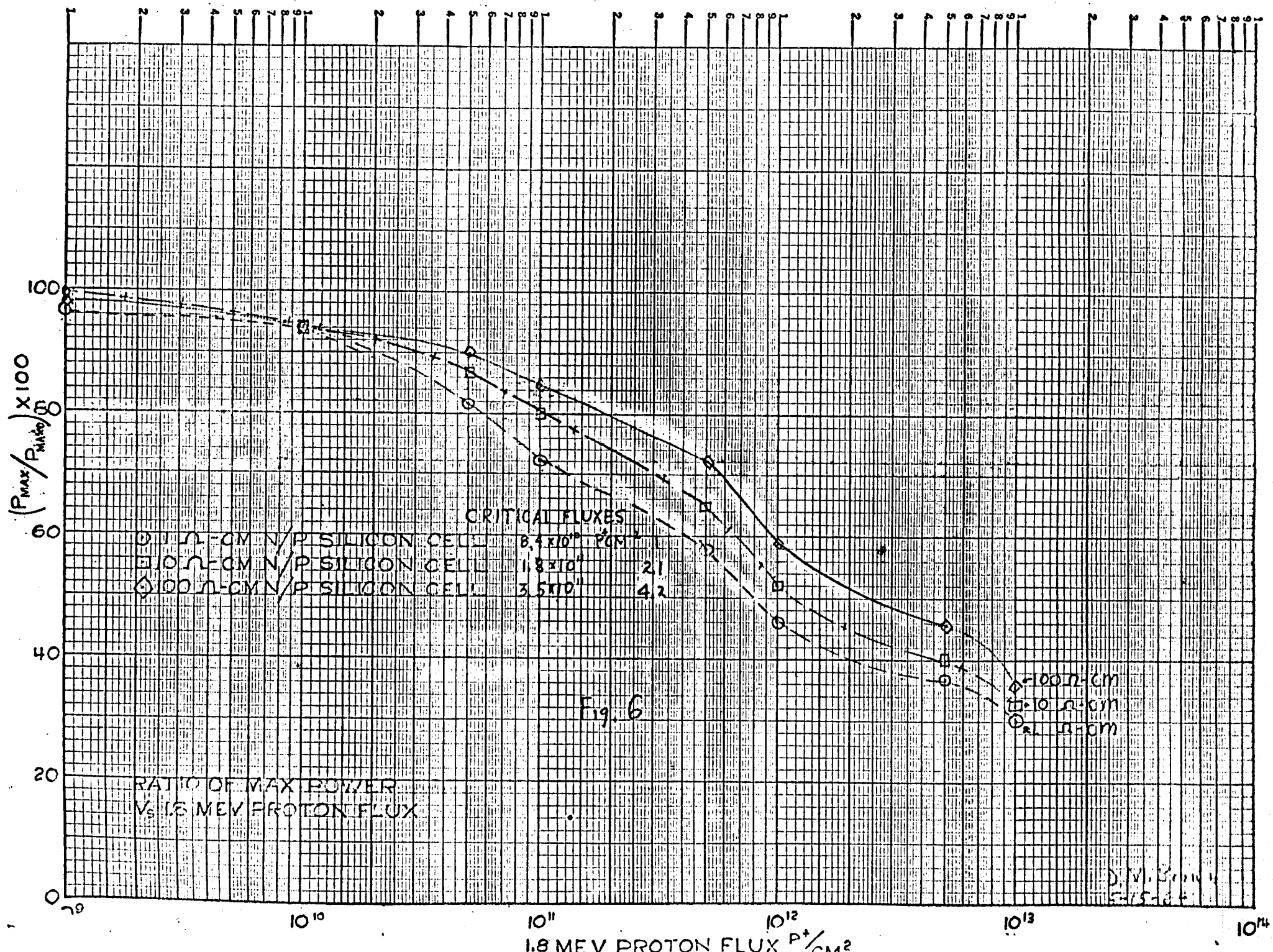

Fig. 6

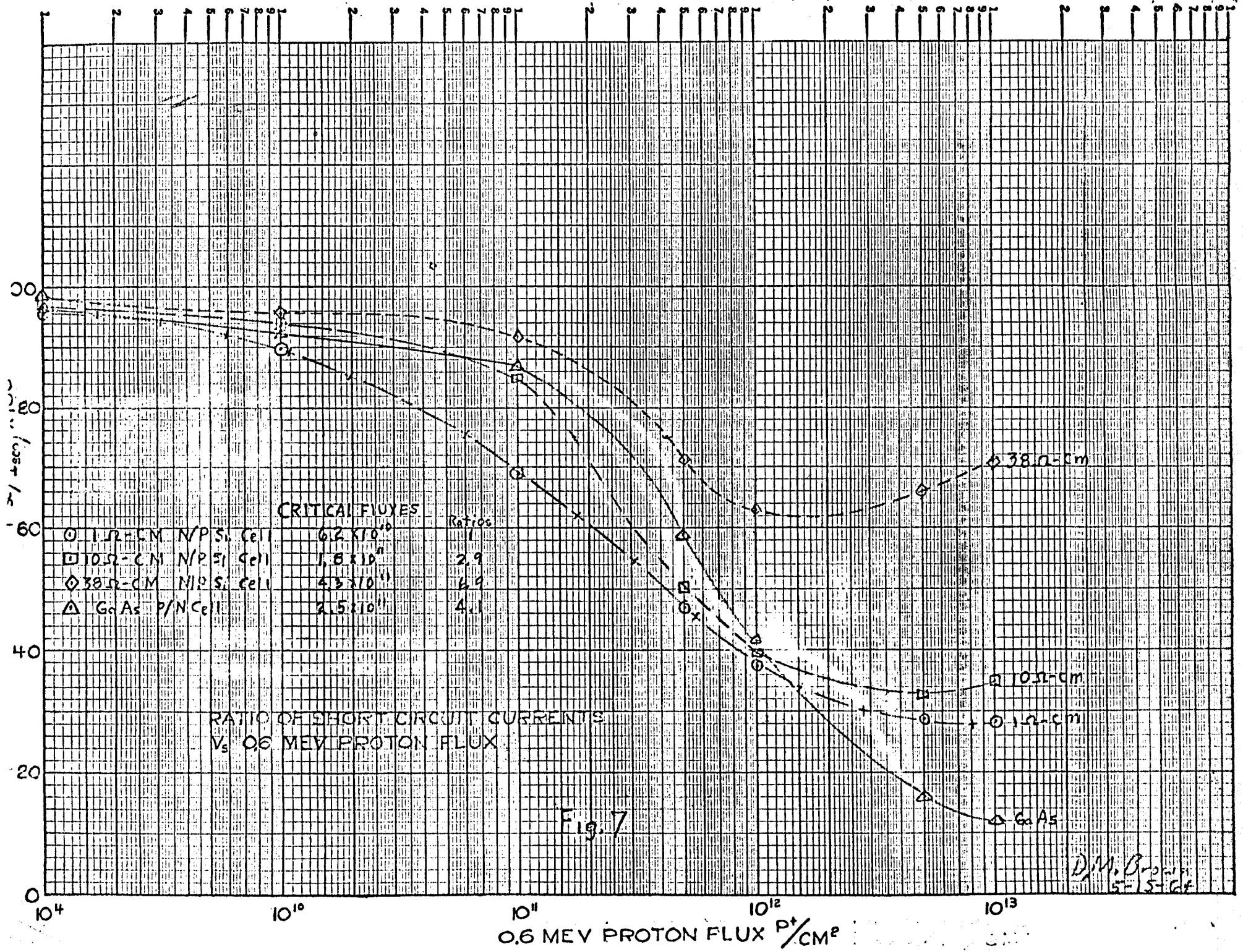

Fig. 7

D.M.B. 5-15-67

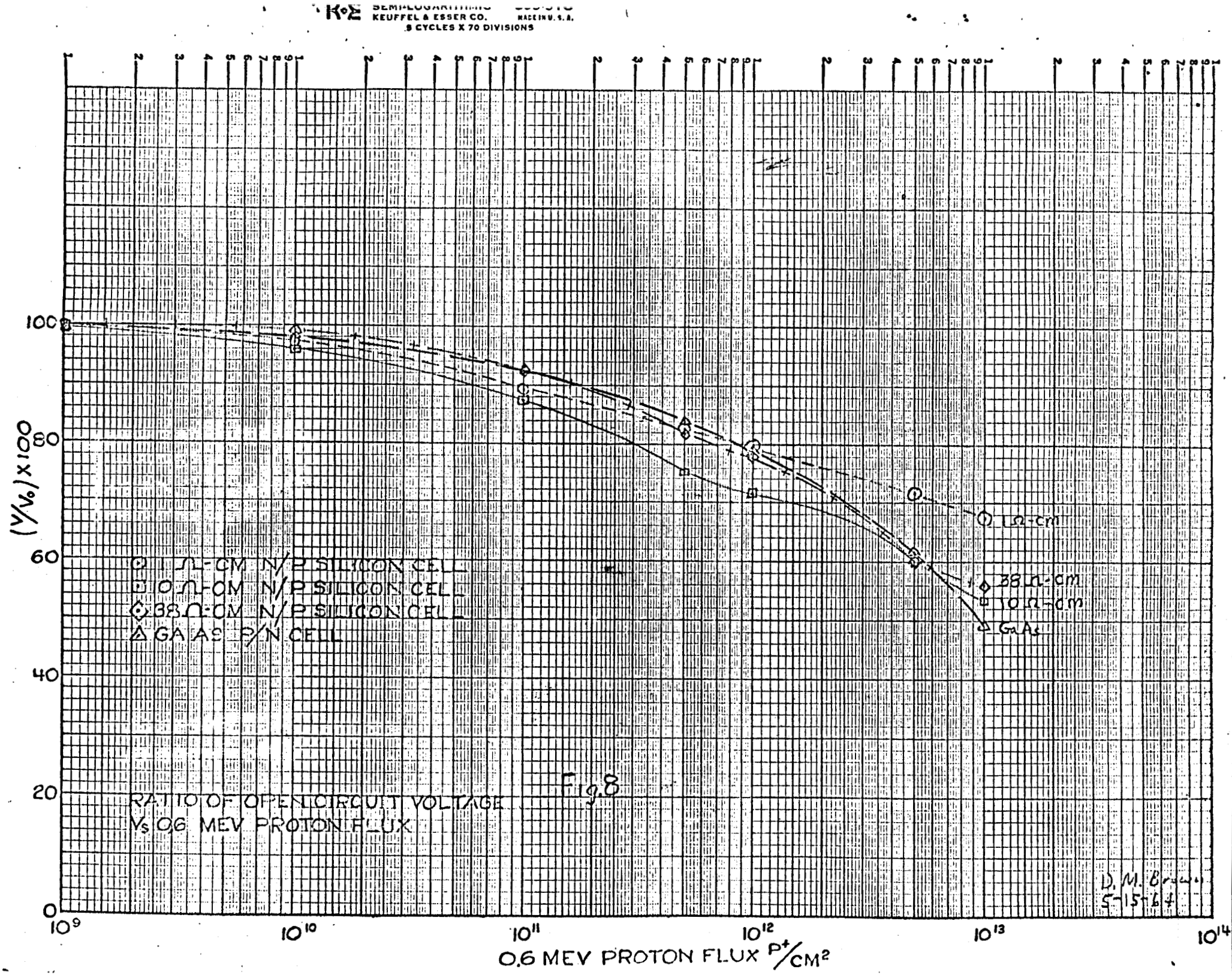

Fig. 8

RATIO OF OPEN CIRCUIT VOLTAGE
Vs 0.6 MEV PROTON FLUX

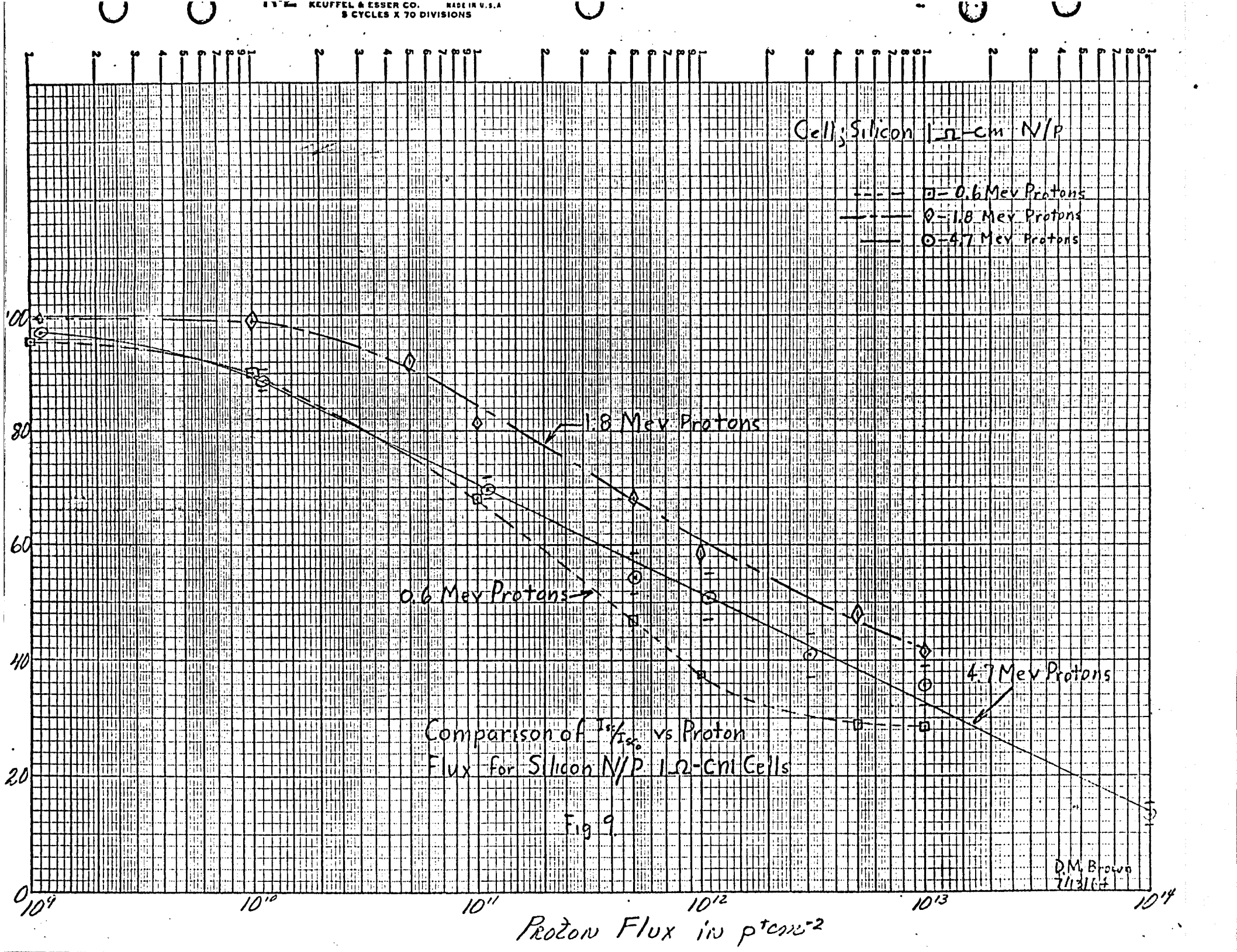

Comparison of I_{sc}/I_{sc_0} vs Proton Flux for Silicon N/P 1 Ω-cm Cells

Fig 9.

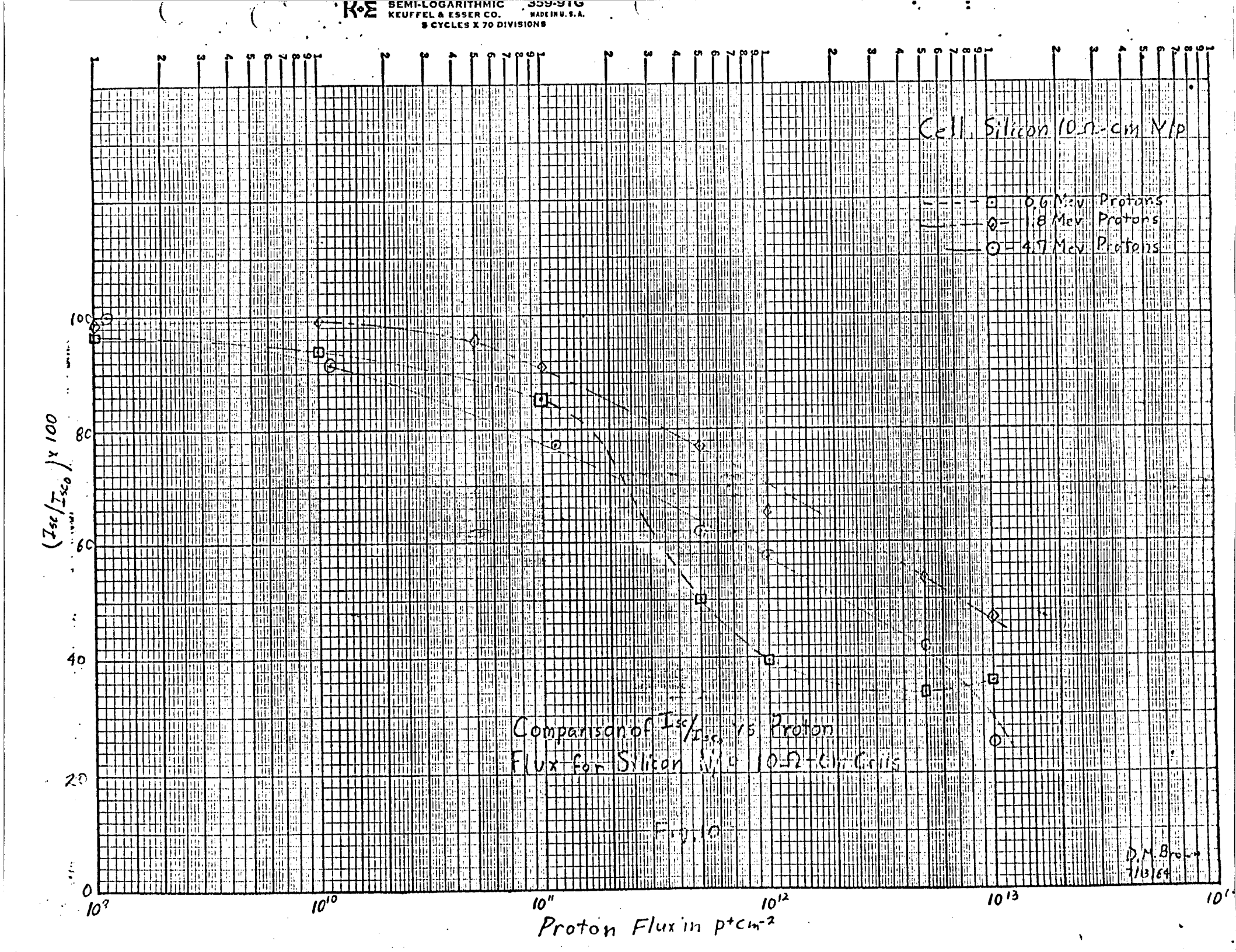
K&E SEMI-LOGARITHMIC 359-91G
KEUFFEL & ESSER CO. MADE IN U.S.A.
5 CYCLES X 70 DIVISIONS
Cell, Silicon 10 Ω-cm N/P
0.6 Mev Protons
1.8 Mev Protons
4.7 Mev Protons
$(I_{sc}/I_{sc_0}) \times 100$
Comparison of I_{sc}/I_{sc_0} vs Proton Flux for Silicon N/P 10-Ω-cm Cells
F-1-1.6
D.M.Brown 7/13/64
Proton Flux in p^+cm^{-2}
0
20
40
60
80
100
10^9
10^{10}
10^{11}
10^{12}
10^{13}

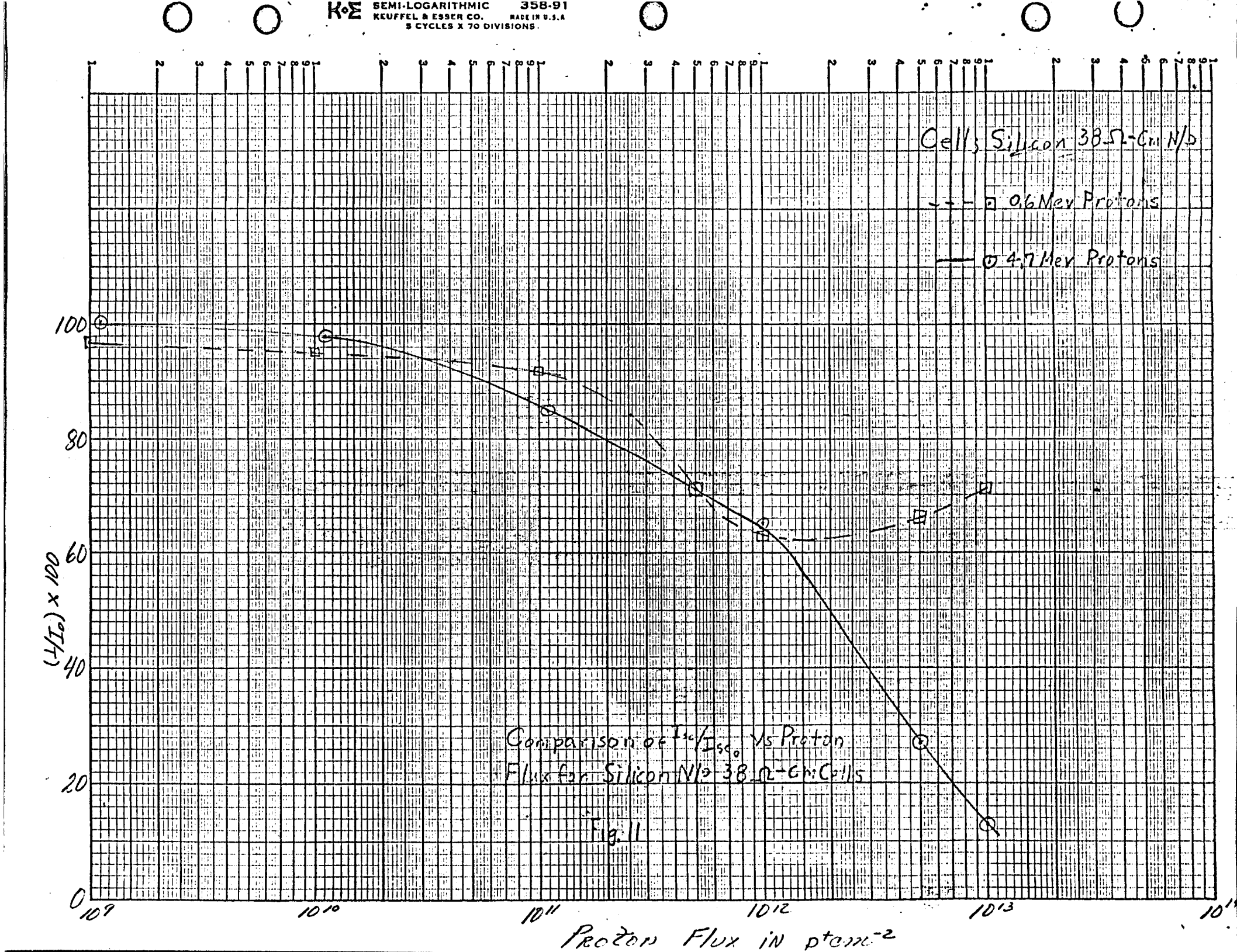
K&E SEMI-LOGARITHMIC 358-91
KEUFFEL & ESSER CO. MADE IN U.S.A.
5 CYCLES X 70 DIVISIONS
Cells Silicon 38 Ω-Cm N/b
0.6 Mev Protons
4.7 Mev Protons
100
80
60
40
20
0
(I/Io) x 100
Comparison of Isc/Isco vs Proton
Flux for Silicon N/2 38 Ω-Cm Cells
Fig. 11
10^9
10^10
10^11
10^12
10^13
Proton Flux in p+cm^-2

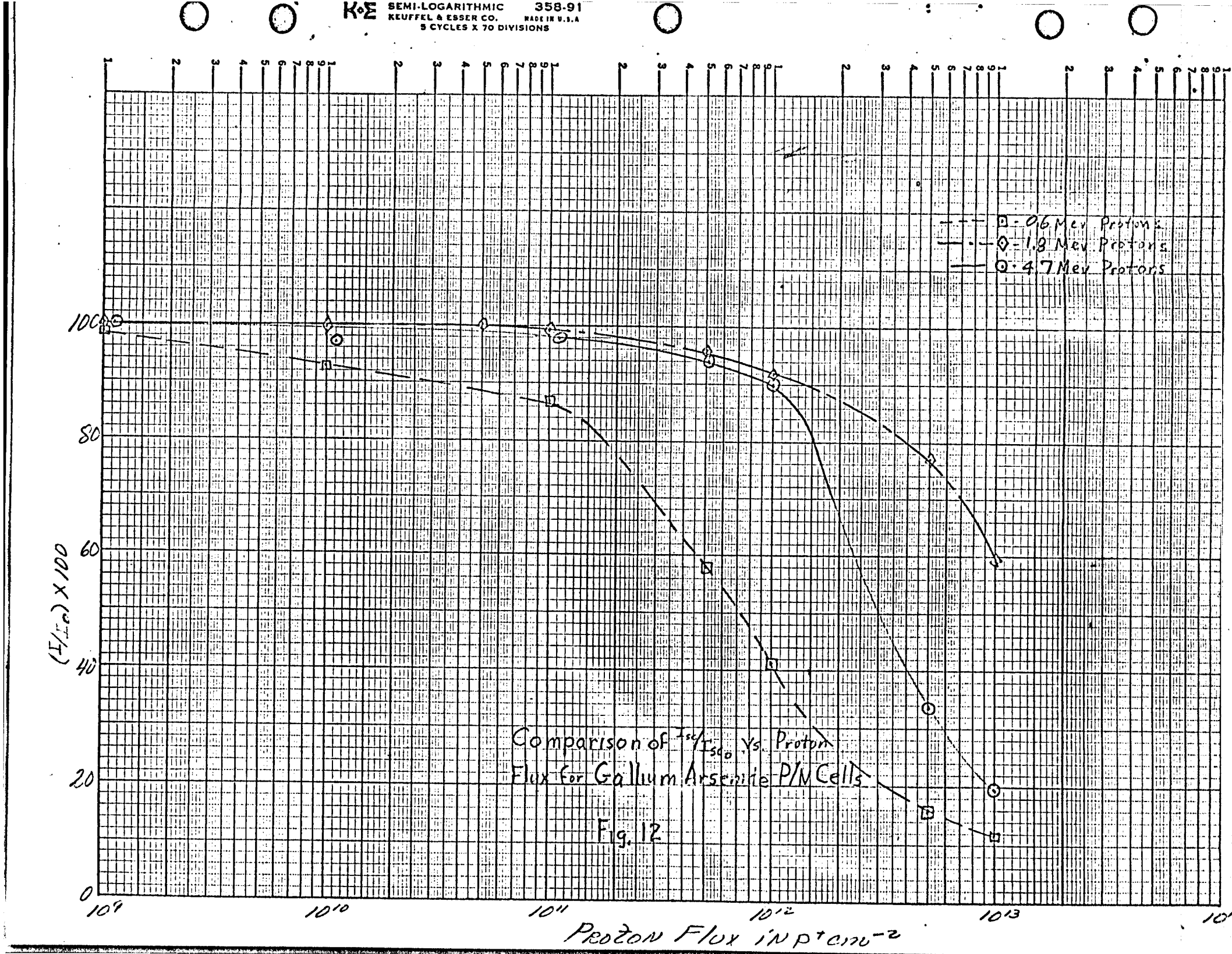
K&E SEMI-LOGARITHMIC 358-91
KEUFFEL & ESSER CO. MADE IN U.S.A
5 CYCLES X 70 DIVISIONS
□ - 0.6 Mev Protons
◇ - 1.8 Mev Protons
○ - 4.7 Mev Protons
100
80
60
40
20
0
(I/Isc) X 100
10⁹
10¹⁰
10¹¹
10¹²
10¹³
Proton Flux in P⁺cm⁻²
Comparison of Isc/Isco Vs. Proton
Flux For Gallium Arsenide P/N Cells
Fig. 12

KEUFFEL & ESSER CO. MADE IN U.S.A.
2 CYCLES X 200 DIVISIONS

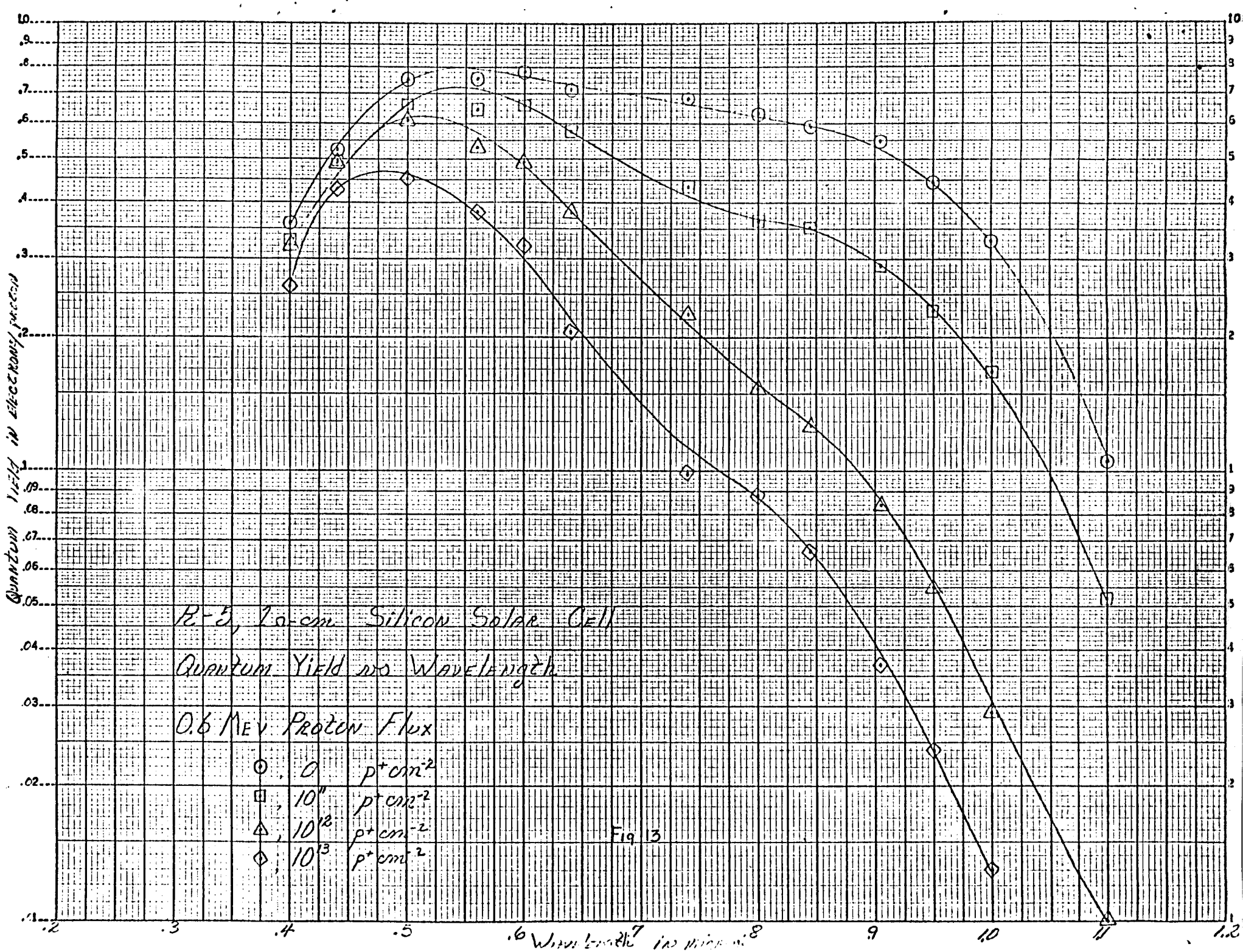

R-E, 1 Ω-cm Silicon Solar Cell

Quantum Yield vs Wavelength

0.6 Mev Proton Flux

○ , 0 $p^+ cm^{-2}$

□ , 10^{11} $p^+ cm^{-2}$

△ , 10^{12} $p^+ cm^{-2}$

◇ , 10^{13} $p^+ cm^{-2}$

Fig 13

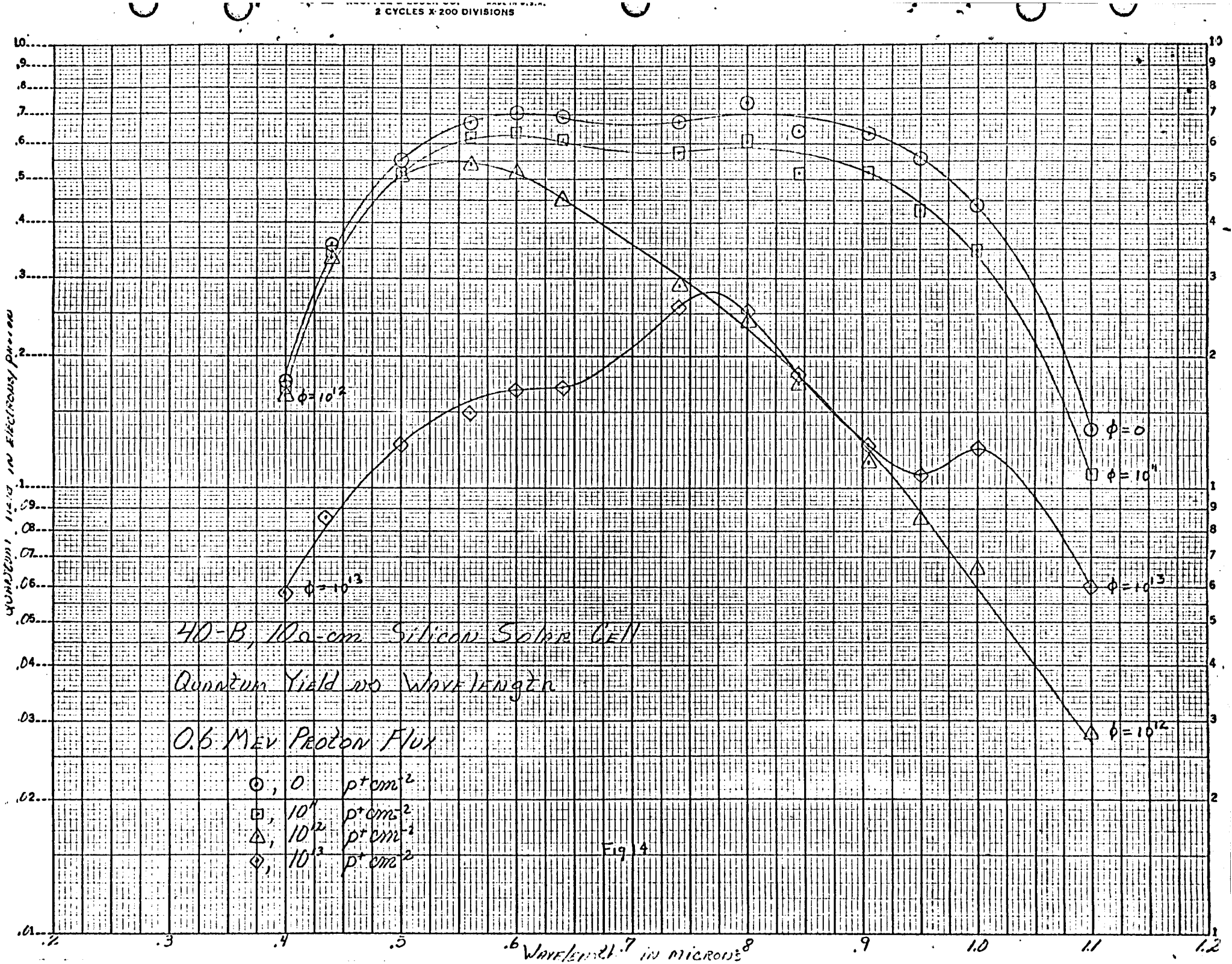
2 CYCLES X 200 DIVISIONS
QUANTUM YIELD IN ELECTRONS/PHOTON
WAVELENGTH IN MICRONS
$\phi = 0$
$\phi = 10^{11}$
$\phi = 10^{12}$
$\phi = 10^{13}$
40-B, 10Ω-cm Silicon Solar Cell
Quantum Yield vs Wavelength
0.6 Mev Proton Flux
⊙, 0 p⁺cm⁻²
□, 10^{11} p⁺cm⁻²
△, 10^{12} p⁺cm⁻²
◇, 10^{13} p⁺cm⁻²

Fig 14

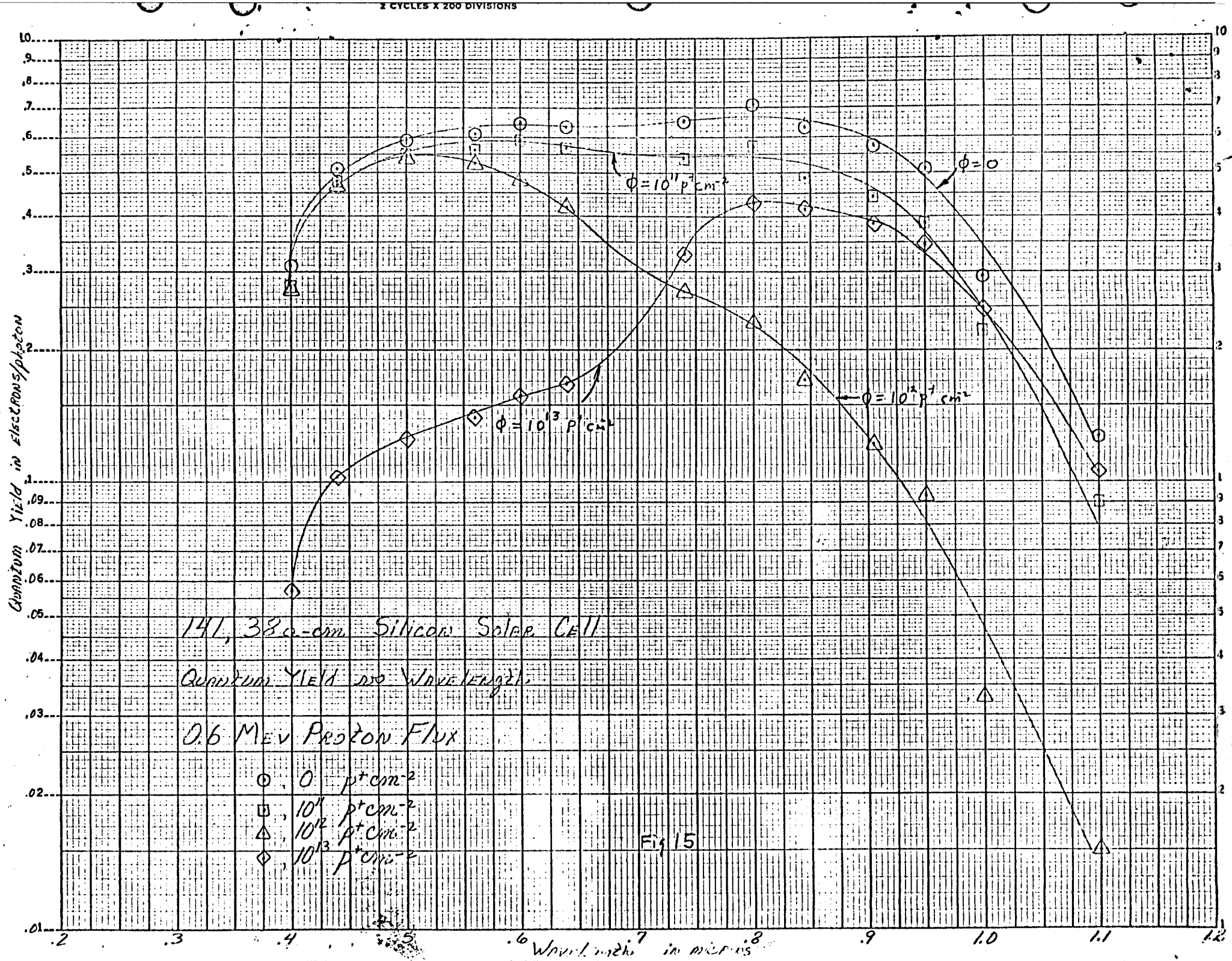
2 CYCLES X 200 DIVISIONS
Quantum Yield in electrons/photon
Wavelength in microns
$\phi = 0$
$\phi = 10^{11}$ p⁺ cm⁻²
$\phi = 10^{12}$ p⁺ cm⁻²
$\phi = 10^{13}$ p⁺ cm⁻²
1.41, 3.8 Ω-cm Silicon Solar Cell
Quantum Yield vs Wavelength
0.6 Mev Proton Flux
○ , 0 p⁺cm⁻²
□ , 10^{11} p⁺cm⁻²
△ , 10^{12} p⁺cm⁻²
◇ , 10^{13} p⁺cm⁻²

Fig 15

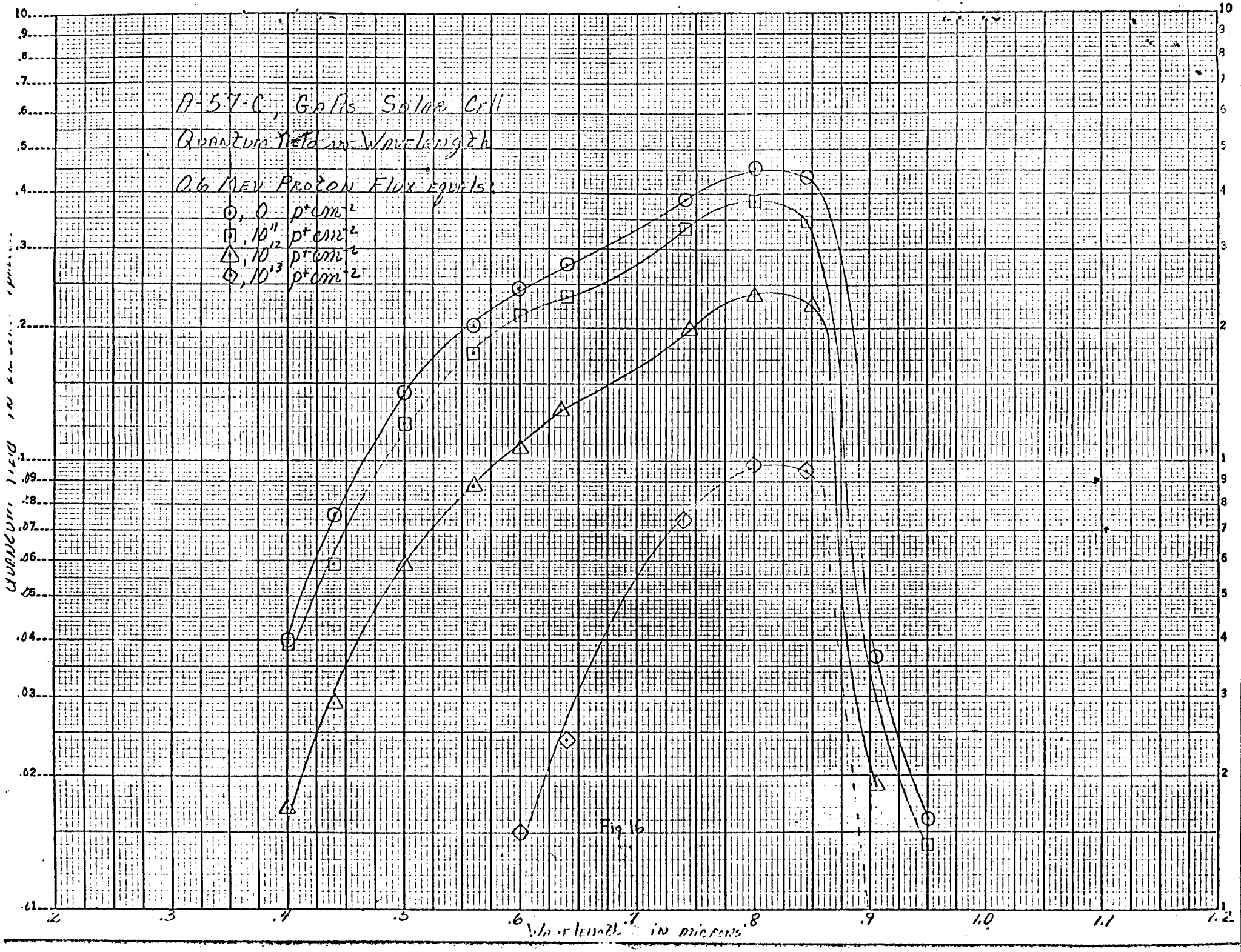
A-57-C, GaAs Solar Cell
Quantum Yield vs. Wavelength
0.6 MEV Proton Flux Equals:
○, 0 p+cm-2
□, 10^11 p+cm-2
△, 10^12 p+cm-2
◇, 10^13 p+cm-2
QUANTUM YIELD IN ELECTRONS PER PHOTON
WAVELENGTH IN MICRONS
.1
.2
.3
.4
.5
.6
.7
.8
.9
1.0
1.1
1.2

Fig 16